

Supporting Information for

**Study of the incorporation and release of the non-conventional half-sandwich ruthenium(II) metallodrug RAPTA-C on a robust MOF**

Elsa Quartapelle Procopio,<sup>a</sup> Sara Rojas,<sup>a</sup> Natalia M. Padial,<sup>b</sup> Simona Galli,<sup>c</sup> Norberto Masciocchi,<sup>c</sup> Fátima Linares,<sup>a</sup> Delia Miguel,<sup>b</sup> J. Enrique Oltra,<sup>b</sup> Jorge A. R. Navarro<sup>a,\*</sup> and Elisa Barea<sup>a,\*</sup>

<sup>a</sup> *Departamento de Química Inorgánica, Universidad de Granada, 18071 Granada, Spain.*

*Fax: (+) 34 958 248526; E-mail: ebaream@ugr.es, jarn@ugr.es*

<sup>b</sup> *Departamento de Química Orgánica, Universidad de Granada, 18071 Granada, Spain.*

<sup>c</sup> *Dipartimento di Scienze Chimiche e Ambientali, Università dell'Insubria, 22100 Como, Italy.*

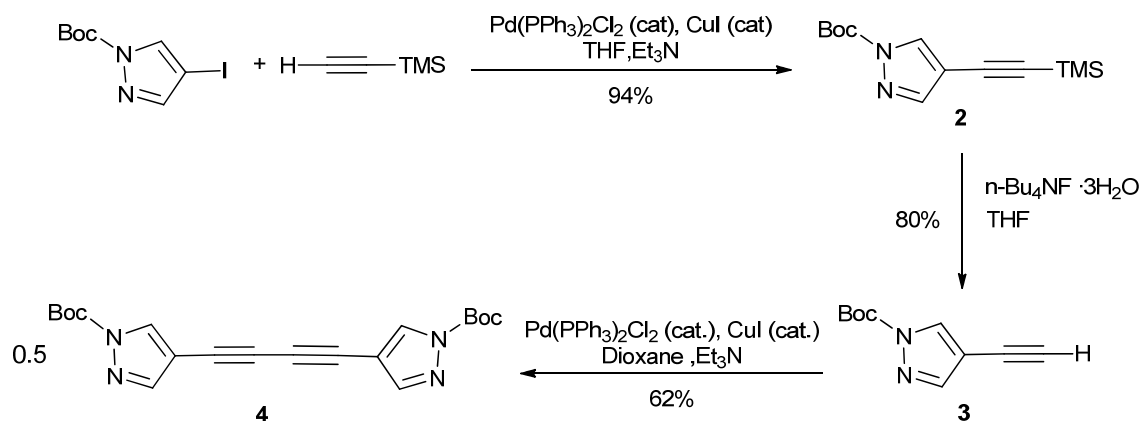
## 1. General methods

General reagents and solvents were commercially available and used as received. [Ru(*p*-cymene)Cl<sub>2</sub>(pta)] (pta = 1,3,5-triaza-7-phosphaadamantane), termed RAPTA-C, was synthesized according to the literature method proposed by C. S. Allardyce *et al. Chem. Commun.*, 2001, 1396. <sup>1</sup>H and <sup>13</sup>C NMR were acquired on a 500 MHz Varian Equipment using CDCl<sub>3</sub> as solvent. Thermogravimetric and differential calorimetric analyses were performed, under air atmosphere, on a Shimadzu-TGA-50H/DSC equipment, at a heating rate of 20 °C min<sup>-1</sup>. UV-vis spectra were collected on a Thermo Unicam UV 300.

Except for the structural analysis, XRPD data were collected on a Bruker D2-PHASER diffractometer using CuK $\alpha$  radiation ( $\lambda = 1.5418 \text{ \AA}$ ). The compounds were manually grounded in an agate mortar, then deposited in the hollow of a silicon sample holder. N<sub>2</sub> adsorption isotherms were measured at 77 K on a Micromeritics Tristar 3000 volumetric instrument. Prior to measurement, powdered samples were activated by heating at 130 °C for 7 h and outgassing to 10<sup>-6</sup> mbar.

## 2. Synthesis

### 2.1. Synthesis of the ligand precursor 1,1'-di-Boc-4,4'-(buta-1,3-diyne-1,4-diyl)bispyrazole (4)



**Scheme S1.** Schematic procedure for the synthesis of boc-1,4-bispyrazolatobut-1,3-diyne (4).

**Preparation of 2:** Commercial 1-boc-4-iodopyrazole (1 g, 3.40 mmol), dichlorobis(triphenylphosphine)palladium(II) (0.24 g, 0.34 mmol) and copper(I) iodide (0.08 g, 0.41 mmol) were stirred in a deoxygenated mixture of Et<sub>3</sub>N (8 mL) and dry THF (10 mL) under an Ar atmosphere for 5 min at room temperature. Subsequently, trimethylsilylacetylene (0.33 g, 3.40 mmol) was slowly added and the mixture was stirred for 3 h. The solvent was removed and the residue was dissolved in ethylacetate (15 mL) and washed with a saturated solution of ammonium chloride (5 mL × 3). The organic phase was dried over anhydrous Na<sub>2</sub>SO<sub>4</sub> and the solvent was removed. The residue was purified by column chromatography (silica gel, hexane/EtOAc 9:1) to yield 0.84 g (94%) of 2 as oil. <sup>1</sup>H NMR (500 MHz, CDCl<sub>3</sub>) δ : 8.15(s, 1H), 7.72 (s, 1H), 1.62 (s, 9H), 0.21 (s, 9H).

**Preparation of 3:** Tetra-*n*-butylammonium fluoride trihydrate (1.03 g, 3.92 mmol) was added to a stirred solution of 2 (0.84 g, 3.26 mmol) in THF (110 mL, *ca.* 0.03 M). The mixture was stirred for 1.5 h at room temperature. Subsequently, the solvent was removed and the residue was dissolved in EtOAc (20 mL). The resulting solution was washed with a saturated aqueous solution of ammonium chloride (8 mL × 3). The

organic phase was dried over anhydrous  $\text{Na}_2\text{SO}_4$  and the solvent was removed. The residue was purified by column chromatography (silica gel, hexane/EtOAc 9:1) to yield 0.60 g (80%) of **3** as oil.  $^1\text{H}$  NMR (500 MHz,  $\text{CDCl}_3$ )  $\delta$  : 8.17 (s, 1H), 7.72 (s, 1H), 3.05 (s, 1H), 1.61 (s, 9H).

**Preparation of 1,1'-di-Boc-4,4'-(buta-1,3-diyne-1,4-diyl)bispyrazole (4):** Terminal alkyne **3** (0.6 g, 3.14 mmol), dichloro-bis(triphenylphosphine) palladium(II) (0.22 g, 0.31 mmol) and copper(I) iodide (0.07 g, 0.38 mmol) were stirred for 4 h at room temperature in a mixture of  $\text{Et}_3\text{N}$  (8 mL) and dioxane (20 mL). Subsequently, the solvent was removed and the residue was dissolved in EtOAc (20 mL). The resulting solution was washed with a saturated aqueous solution of ammonium chloride (5 mL  $\times$  3). Afterwards, the organic phase was dried over anhydrous  $\text{Na}_2\text{SO}_4$  and the solvent was removed. The resulting residue was purified by column chromatography (silica gel, hexane/EtOAc 8:2) to yield 0.37 g (62%) of **4** as white needles. IR (KBr)  $\tilde{\nu}$  ( $\text{cm}^{-1}$ ): 2160, 1660.  $^1\text{H}$  NMR (500 MHz,  $\text{CDCl}_3$ )  $\delta$ : 8.25 (s, 2H), 7.79 (s, 2H), 1.65 (s, 18H).  $^{13}\text{C}$  NMR (126 MHz,  $\text{CDCl}_3$ ) (DEPT)  $\delta$ : 146.6 (C), 146.0 (CH), 134.5 (CH), 105.2 (C), 86.5 (C), 76.1 (C), 71.5 (C), 27.9 ( $\text{CH}_3$ ). HRMS (ESI) calculated for  $\text{C}_{20}\text{H}_{22}\text{N}_4\text{O}_4\text{Na}$ : 405.1539, found: 405.1532.

## NMR spectroscopy for **4**

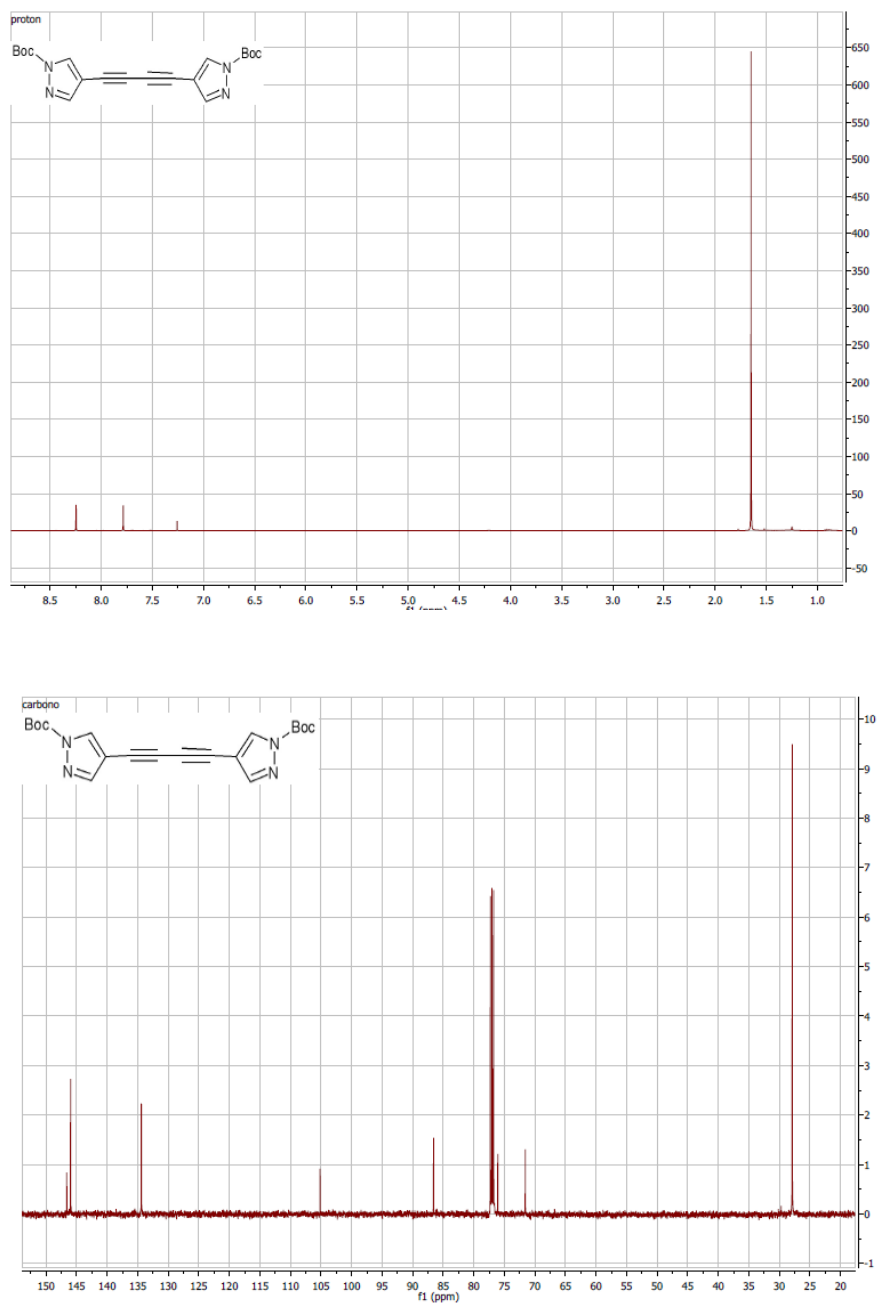


**Figure S1.**  $^1\text{H}$  NMR (top) and  $^{13}\text{C}$  NMR (bottom) for 1,1'-di-Boc-4,4'-(buta-1,3-diyne-1,4-diyl)bispyrazole (**4**).

## 2.2. Synthesis of $[\text{Ni}_8(\text{OH})_4(\text{OH}_2)_2(1,4\text{-bispyrazolatobut-1,3-diyne})_6] (\text{H}_2\text{O})_{11} (\text{C}_3\text{H}_7\text{NO})_{13} (1 \cdot \text{H}_2\text{O} \cdot \text{DMF})$

In a typical synthesis, 105.6 mg (0.3 mmol) of boc-1,4-bispyrazolatobut-1,3-diyne were dissolved in 16 mL of DMF and 99.2 mg (0.4 mmol) of  $\text{Ni}(\text{AcO})_2 \cdot 4\text{H}_2\text{O}$  were dissolved in 4 mL of  $\text{H}_2\text{O}$ . The two limpid solutions were mixed together and refluxed for 6 h under stirring. The light green solid obtained was filtered and washed with EtOH and  $\text{Et}_2\text{O}$ , yielding 95 mg of  $[\text{Ni}_8(\text{OH})_4(\text{OH}_2)_2(1,4\text{-bispyrazolatobut-1,3-diyne})_6] \cdot (\text{H}_2\text{O})_{11} \cdot (\text{DMF})_{13}$  (yield: 80.3%). Anal. calc. for  $[\text{Ni}_8(\text{OH})_4(\text{OH}_2)_2(\text{C}_{10}\text{N}_4\text{H}_4)_6] \cdot (\text{H}_2\text{O})_{11} (\text{C}_3\text{H}_7\text{NO})_{13}$  C, 42.24; H, 5.21; N, 18.49; found. C, 42.68; H, 5.21; N, 17.98.

## 3. Thermal analysis on $1 \cdot \text{H}_2\text{O} \cdot \text{DMF}$ and $\text{CH}_2\text{Cl}_2$ exchanged $1 \cdot \text{CH}_2\text{Cl}_2$

The as synthesized solid,  $1 \cdot \text{H}_2\text{O} \cdot \text{DMF}$ , was suspended in  $\text{CH}_2\text{Cl}_2$  for 4 h to exchange the host solvent molecules in order to decrease the activation/evacuation temperature.

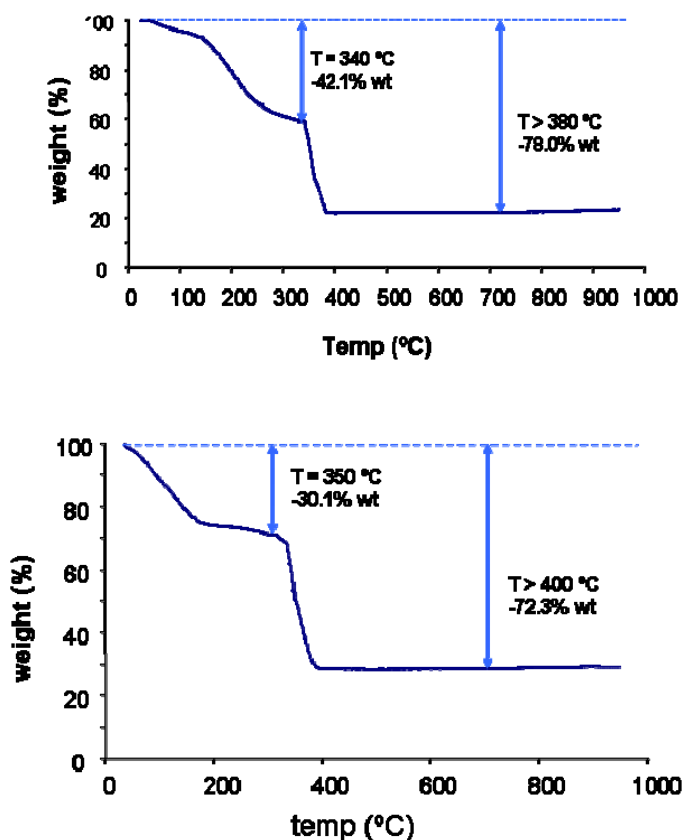
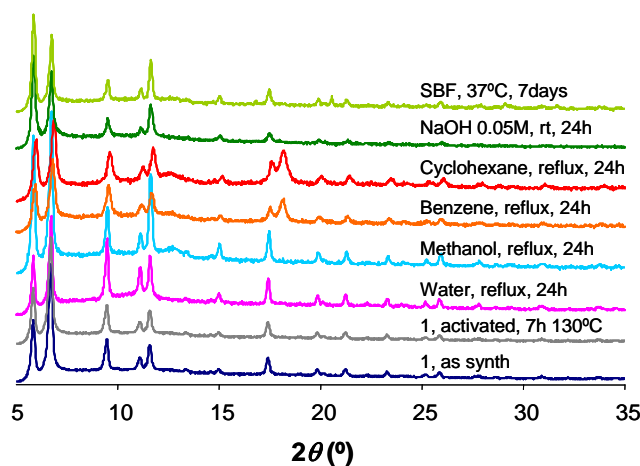


**Figure S2.** TG trace for  $1 \cdot \text{H}_2\text{O} \cdot \text{DMF}$  (top) and  $\text{CH}_2\text{Cl}_2$  exchanged  $1 \cdot \text{CH}_2\text{Cl}_2$  (bottom) under air atmosphere.

#### 4. Chemical stability tests on 1

Each test has been performed suspending 20 mg of activated **1** into 10 mL of the desired solvent for 24h. Afterwards, the solid was filtered off and dried 1h in air at room temperature before XRPD acquisition.

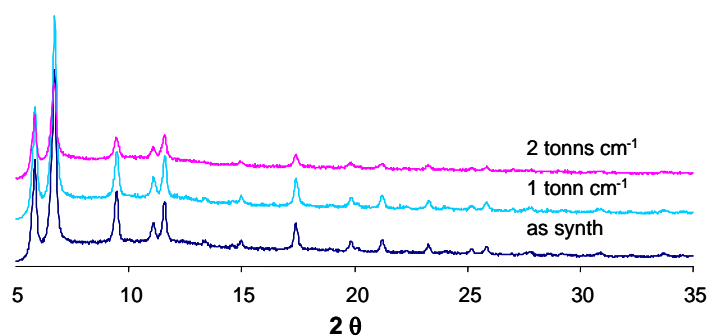
It should be highlighted that the bulk solid is stable in acid conditions (HCl 0.01M, pH 2.3, 24h, rt) as its XRPD is not affected after this treatment and its crystallinity is maintained. However, it should be pointed out that the quantity of recovered solid after the treatment seems to be diminished suggesting that the MOF is progressively leached under these conditions.



**Figure S3.** XRPD patterns acquired on species **1** as synthesized, activated and after different chemical stability tests.

#### 5. Mechanical stability tests on 1

A typical test consisted in the characterization, by XRPD and  $N_2$  adsorption at 77 K, of pellets obtained by applying pressure ( $1 \text{ Mg cm}^{-2}$  and  $2 \text{ Mg cm}^{-2}$ ) to 100 mg of the original sample during 60 seconds. In order to register the XRP diffractograms and to measure the  $N_2$  adsorption at 77 K, the pellets were gently grounded in an agate mortar.



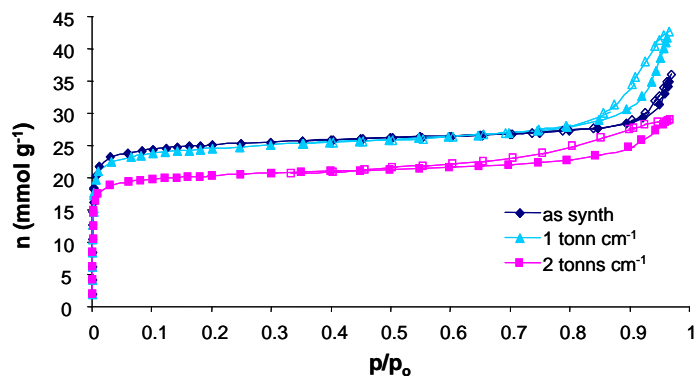


**Figure S4.** Top: XRPD data for **1**. Bottom: N<sub>2</sub> adsorption isotherms for the activated form, **1**, before and after the mechanical stress tests. Desorption branches of the isotherms are depicted with empty symbols.

## 6. Adsorption and release of RAPTA-C from activated **1**

The amount of RAPTA-C in solution was checked by UV-vis. The UV-vis maximum absorption band for RAPTA-C in distilled water is found at 323 nm with a tail peak at about 400 nm. These peaks essentially belong to [Ru(p-cymene)Cl(H<sub>2</sub>O)(pta)] complex that is quickly obtained when RAPTA-C is hydrolyzed in water.<sup>1</sup> In SBF these two maxima shift to 300 nm and 384 nm respectively.

The eventually leached ligand is not soluble either in water or in SBF, so that any impurity of free bispyrazolate ligand cannot interfere the UV-vis absorption of the RAPTA-C species.

**Evacuation of 1:** Prior the measurement of the adsorption isotherm of RAPTA-C into **1**, the as synthesized solid **1**·H<sub>2</sub>O·DMF (200 mg) was suspended in 100 mL of CH<sub>2</sub>Cl<sub>2</sub> for 4 hours to ensure the complete exchange of the guest solvent molecules (H<sub>2</sub>O and DMF) with more volatile CH<sub>2</sub>Cl<sub>2</sub> guests. Afterwards, powdered samples of **1**·CH<sub>2</sub>Cl<sub>2</sub> were heated at 130 °C for 7 h and outgassed to 10<sup>-6</sup> mbar. Under these conditions, the complete removal of the guest molecules in order to obtain empty pores ready for RAPTA-C adsorption could be achieved.

**Measurement of the adsorption isotherm of RAPTA-C at 298 K:** RAPTA-C solutions were prepared using increasing concentrations of RAPTA-C by dissolving 5,



10, 20, 30, 35, 40, 50, 65, 80 mg of RAPTA-C in 5 ml of water (Milli-Q distilled water) stirring overnight at room temperature ( $[RAPTA-C]_0 = 0.0022, 0.0043, 0.0086, 0.0129, 0.0151, 0.0173, 0.0216, 0.0281, 0.0345$  M). RAPTA-C solid-liquid adsorption isotherm was measured at 298 K by suspending 10 mg of activated **1** in the RAPTA-C aqueous solutions under stirring for 4 h in order to assure that equilibrium was reached. Then, each sample was centrifuged, by means of a Sigma 3-30K centrifuge, using centrifuge tubes with a 30 kDa PES filter, at 8000 rpm for 10 minutes to achieve the separation of **1**·RAPTA-C matrix from the solution. The amount of RAPTA-C incorporated into **1** was indirectly calculated monitoring, by means of UV-vis, the decrease of RAPTA-C concentration from the filtered solution. Using the Lambert-Beer law, the concentration of RAPTA-C in solution was calculated from the maximum absorbance peak at 323 nm. Taking into account the initial amount of RAPTA-C in the solution, it is possible to calculate the amount of RAPTA-C incorporated in **1**.

**Release of RAPTA-C:** The delivery of RAPTA-C in simulated body fluid (SBF) at 323 K has been studied. SBF was prepared according to literature methods.<sup>2</sup> With this purpose, we prepare two solutions, A and B (Table S1), that must be mixed just before each experiment in order to avoid the possible precipitation of some low soluble inorganic salts.

	Sol. A (g/L)	Sol. B (g/L)
NaCl	6.213	6.213
NaHCO <sub>3</sub>	5.948	
KCl	0.450	
Na <sub>2</sub> HPO <sub>4</sub> ·2H <sub>2</sub> O		0,498
K <sub>2</sub> HPO <sub>4</sub> ·3H <sub>2</sub> O	0.462	
MgCl <sub>2</sub> ·6H <sub>2</sub> O	0.622	
CaCl <sub>2</sub>		0.584
Na <sub>2</sub> SO <sub>4</sub>	0.144	

**Table S1.** Composition of the A and B solutions used for the preparation of simulated body fluid.

The metallodrug delivery process was studied by suspending 10 mg of activated **1**·RAPTA-C in SBF, incubated at 37 °C, under stirring. Aliquots (2 mL) of the supernatant solution were analyzed by means of UV-vis ( $\lambda = 323$  nm) at different

periods of time (10, 20, 30, 45, 60 min, 2, 4, 6, 8, 12, 24 h) in order to determine the amount of desorbed RAPTA-C and the kinetics of the process. The solutions were filtered using centrifuge tubes with a 30 kDa PES filter, at 8000 rpm for 2 minutes, then both the solution and the solid were joined to the mother solution to keep the volume constant.

Furthermore, we studied the reversibility of the desorption process quantifying the quantity of RAPTA-C delivered after reaching the equilibrium. First of all, a suspension of 10 mg of **1**·RAPTA-C in 10 mL of SBF was sonicated for 90 minutes. Then, the volume was increased up to 200 mL with fixed steps ( $V_{\text{tot}} = 20, 30, 50, 75, 100, 150, 200$  mL) and the same treatment was performed after each addition. Aliquots (2 mL) of the supernatant solution were studied by means of UV-vis ( $\lambda = 323$  nm) to determine the amount of released RAPTA-C.

## 7. X-ray powder diffraction of **1** and **1**·RAPTA-C

The loaded form **1**·RAPTA-C has been obtained suspending 10 mg of activated **1** into 20 mL of an aqueous RAPTA-C solution (0.025 M), stirring at 25° C for 4 hours to ensure that the equilibrium is reached. The solid was filtered, washed quickly with 1 mL of distilled water and dried under reduced pressure.

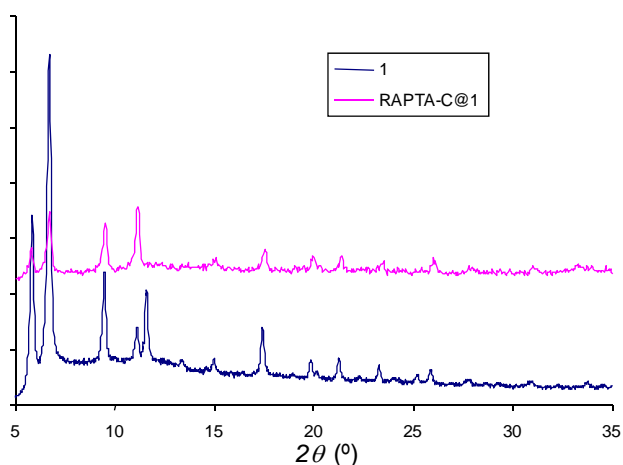


**Figure S5.** XRPD patterns acquired on activated (**1**) and loaded RAPTA-C species (**1**·RAPTA-C)

**8. X-ray powder diffraction structural analysis on **1**·H<sub>2</sub>O·DMF.** A microcrystalline batch of **1**·H<sub>2</sub>O·DMF was gently ground in an agate mortar, and then was deposited in

the hollow of an aluminum sample holder equipped with a zero-background plate. Diffraction data were collected by means of an overnight scan in the  $2\theta$  range of  $5\text{-}105^\circ$ , with  $0.02^\circ$  steps, on a Bruker AXS D8 Advance diffractometer, equipped with Ni-filtered Cu-K $\alpha$  radiation ( $\lambda = 1.5418 \text{ \AA}$ ) and with a Lynxeye linear position-sensitive detector, and mounting the following optics: primary beam Soller slits ( $2.3^\circ$ ), fixed divergence slit ( $0.5^\circ$ ), receiving slit (8 mm). The generator was set at 40 kV and 40 mA. A visual inspection of the acquired diffractogram allowed to purport isomorphism between **1·H<sub>2</sub>O·DMF** and the  $[\text{Ni}_8(\mu_4\text{-OH})_4(\mu_4\text{-OH}_2)_2(\mu_4\text{-L})_6]_n \cdot n\text{Solv}$  systems,<sup>3</sup> as confirmed by independent indexing. Standard peak search, followed by indexing through the Single Value Decomposition approach<sup>4</sup> implemented in TOPAS-R,<sup>5</sup> allowed the detection of the approximate unit cell parameters of **1·H<sub>2</sub>O·DMF**. The lattice F-centering was assigned on the basis of the systematic absences, and the space group chosen taking into consideration the purported isomorphism. Unit cell and space group were checked by Le Bail refinements and later confirmed by structure solution and refinement. The structure solution was performed by the simulated annealing technique, as implemented in TOPAS, employing a rigid, idealized model for the crystallographic independent portion of the ligand.<sup>6</sup> The difference Fourier map calculated with the  $F_c$ s of the framework alone revealed that the solvent is highly disordered. Its electronic density was modeled by locating, within the cavities, the number of oxygen atoms whose refined site occupation factors, combined with the site multiplicity, represent the total electron density of the solvent, as estimated from the elemental and TG analyses. The presence of dynamic disorder was taken into account by assigning to these atoms a high isotropic thermal parameter, corresponding to a mean square displacement of  $0.9 \text{ \AA}^2$ . The final refinement was carried out by the Rietveld method, maintaining the rigid body introduced at the solution stage. The background was modeled by a polynomial function. One, refinable, isotropic thermal parameter was attributed to the metal atoms ( $B_M$ ), lighter atoms (with the notable exception cited above) being given a  $B_{\text{iso}} = B_M + 2.0 \text{ \AA}^2$  value. Peak shapes were described by the Fundamental Parameters Approach.<sup>7</sup>

Crystal data for **1·H<sub>2</sub>O·DMF**:  $[\text{Ni}_8(\text{OH})_4(\text{OH}_2)_2(\text{C}_{10}\text{N}_4\text{H}_4)_6] \cdot (\text{H}_2\text{O})_{11} \cdot (\text{C}_3\text{H}_7\text{NO})_{13}$ ,  $f_w = 2803.0 \text{ g mol}^{-1}$ , cubic,  $Fm\text{-}3m$ ,  $a = 26.4908(7)$ ,  $V = 18590(1) \text{ \AA}^3$ ,  $Z = 4$ ,  $\rho = 1.00 \text{ g cm}^{-3}$ ,

$\mu(\text{Cu-K}\alpha) = 14.2 \text{ mm}^{-1}$ ,  $R_p$ ,  $R_{wp}$  and  $R_{Bragg} = 0.016, 0.022, 0.010$ , respectively, for 5001 data collected in the  $5.0\text{-}105.0^\circ 2\theta$  range.

Fractional atomic coordinates are supplied in the Supporting Information as a CIF file. X-ray crystallographic data in CIF format have been deposited with the Cambridge Crystallographic Data Center as supplementary publication no. 829304. Copies of the data can be obtained free of charge on application to the Director, CCDC, 12 Union Road, Cambridge, CB2 1EZ, UK (Fax: +44-1223-335033; e-mail: deposit@ccdc.cam.ac.uk or <http://www.ccdc.cam.ac.uk>).

### 9. Pore size distribution on 1.

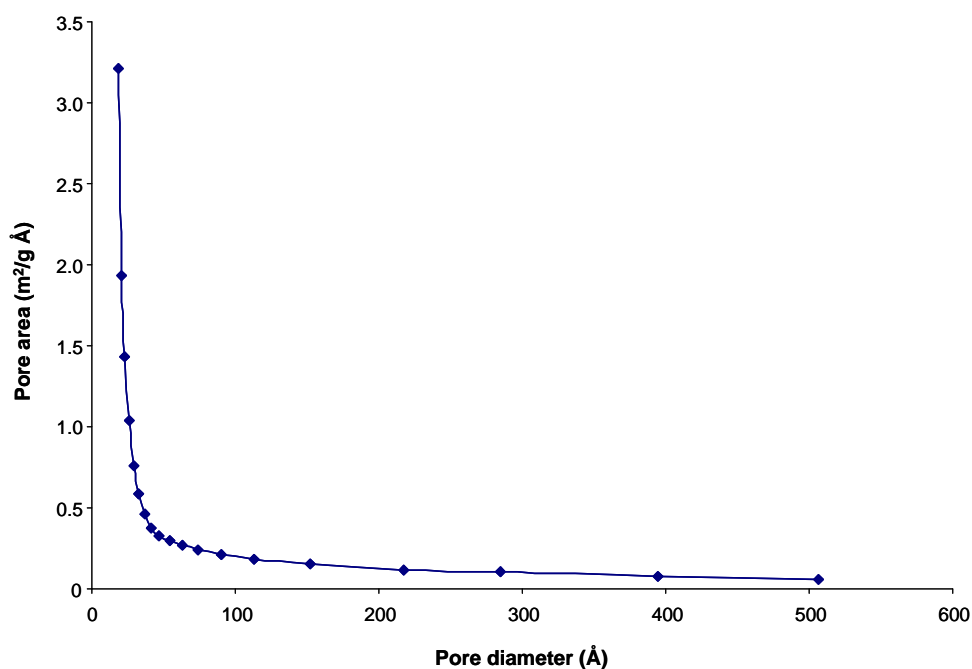


**Figure S6.** Pore size distribution was calculated using the BJH method. As it can be observed the pore size is in the microporous range (pore size  $\leq 1.5 \text{ nm}$ ).

## References

---

- <sup>1</sup> C. Scolaro, C. G. Hartinger, C. S. Allardyce, B. K. Keppler and P. J. Dyson, *J. Inorg. Chem.* 2008, **102**, 1743.
- <sup>2</sup> T. Kokubo, H. Kushitani, C. Ohtsuki, S. Sakka, and T. Yamamuro, *J. Mater. Sci.: Mater. Med.*, 1992, **3**, 79.
- <sup>3</sup> N. Masciocchi, S. Galli, V. Colombo, A. Maspero, G. Palmisano, B. Seyyedi, C. Lamberti and S. Bordiga, *J. Am. Chem. Soc.*, 2010, **132**, 7902.
- <sup>4</sup> A. Coelho, *J. Appl. Cryst.* 2003, **36**, 86.
- <sup>5</sup> TOPAS Version 3.0, Bruker AXS **2005**, Karlsruhe, Germany.
- <sup>6</sup> To describe the crystallographically independent portion of the ligand, a rigid model was adopted imposing idealized bond distances and angles as follows: C-C, C-N, N-N of the heterocyclic ring 1.36 Å; single C-C 1.40 Å; triple C-C 1.25 Å; C-H 0.95 Å; heterocyclic ring internal bond angles 108°.
- <sup>7</sup> R. W. Cheary and A. Coelho, *J. Appl. Cryst.* 1998, **31**, 85; *ibid.* 862.